energies

MDPI

Article

A Novel Exergy Indicator for Maximizing Energy Utilization in Low-Temperature ORC

Marcin Jankowski [1,*] and Aleksandra Borsukiewicz [1,2]

[1] ORC Power Plants Research and Development Centre, West Pomeranian University of Technology in Szczecin, al. Piastów 17, 70-310 Szczecin, Poland; aborsukiewicz@zut.edu.pl
[2] School of Mechanical & Mining Engineering, The University of Queensland, Queensland 4072, Australia
* Correspondence: marcin.jankowski@zut.edu.pl

Received: 27 February 2020; Accepted: 19 March 2020; Published: 1 April 2020

Abstract: In the last decade, particular attention has been paid to the organic Rankine cycle (ORC) power plant, a technology that implements a classical steam Rankine cycle using low-boiling fluid of organic origin. Depending on the specific application and the choice of the designer, the ORC can be optimized using one or several criteria. The selected objectives reflect various system performance aspects, such as: thermodynamic, economic, environmental or other. In this study, a novel criterion called exergy utilization index (*XUI*) is defined and used to maximize the utilization of an energy source in the ORC system. The maximization of the proposed indicator is equivalent to bring the heat carrier outlet temperature to the ambient temperature as close as possible. In the studied case, the *XUI* is applied along with the total heat transfer area of the system, and the multi-objective optimization is performed in order to determine the optimal operating conditions of the ORC. Moreover, to reveal a relationship between the *XUI* and important ORC performance indicators, a parametric study is conducted. Based on the results, it has been found that high values of the *XUI* (~80%) correspond to optimal values of exergy-based indicators such as: exergy efficiency, waste exergy ratio, environmental effect factor or exergetic sustainability index. Furthermore, the values of the *XUI* = 60%–80% are associated with beneficial economic characteristics reflected in a low payback period (<11.3 years). When considering the ecological aspect, the maximization of *XUI* has resulted in minimization of exergy waste to the environment. In general, the simple formulation and straightforward meaning make the *XUI* a particularly useful indicator for the preliminary evaluation and design of the ORC. Furthermore, the comparative analysis with respect to other well-known performance indicators has shown that it has a potential to be successfully applied as the objective function in the optimization of ORC power plants.

Keywords: ORC; multi-objective optimization; exergy; genetic algorithm; energy utilization

1. Introduction

The global increase in the demand for electricity necessitates the search for alternative energy sources and the development of technologies that can efficiently convert this type of energy into electricity. The organic Rankine cycle (ORC) seems to be the optimal choice for that purpose, since it allows for the utilization of low and medium-temperature heat carriers, such as: geothermal water, exhaust gases, thermal oils etc. One way to characterize an energy source for the ORC is to classify it as one of the two types: closed (sealed) or open [1]. The first type is characterized by a constant temperature of the heat carrier exiting the vapor generator of the ORC. This occurs in applications in which the heat carrier is circulating in a closed loop and it must have a predefined temperature at the outlet of the heat exchanger. In the case of the second type, the heat carrier leaving the vapor generator is directed to the environment and its outlet temperature does not have a pre-determined value. Such

systems are distinguished by the fact that they can be optimized by minimizing the heat carrier outlet temperature as far as possible [2]. This is equivalent to maximize the heat source potential which has been shown to improve the ORC performance by reducing the exergy waste to the environment [3].

The aspect of an efficient utilization of the energy source is not addressed directly in most studies. Moreover, in the case of closed type energy sources, the maximization of their potential is not even possible, since the outlet temperature of the heat carrier is fixed, and the heat transferred in the vapor generator cannot be increased. For the open type energy source, an investigation which aims to evaluate the heat carrier utilization degree is conducted by several authors. Garg and Orosz [4] applied the effectiveness ε, an energy-based indicator, in order to recover the maximum available waste heat in the ORC. The ε is a ratio of the actual heat transferred by a heat carrier to the maximum available heat which would be released by cooling the heat carrier to the ambient temperature. The authors combined the ε with the economic criterion to construct a novel objective function that maximizes the waste energy potential and minimizes the cost of the system. The effectiveness index ε was also used by Li et al. [5] in parametric optimization of single and dual-pressure evaporation ORCs. In their study, the indicator was applied to compare the energy utilization results for two heat carriers—hot water and hot air.

The exergy analysis provides mathematically defined indicators which are used to assess the sustainable performance of the ORC [6]. In other words, the exergy-based indices are developed in a way that evaluates the system from the perspectives of its economic viability and environmental impact. The first objective may be achieved by applying indicators that maximize the power output of the ORC. To attain the second goal, the exergy losses of the system should be reduced as much as possible [7]. By decreasing the exergy waste to the environment, the heat carrier utilization can be maximized. For that reason, the exergy analysis seems to be an appropriate tool for optimizing the energy source utilization.

The definitions of exergy indicators which hold for a basic ORC (see Figure 1) are presented in Equations (1)–(5). The exergy efficiency η_{ex} [8] is one of the most often utilized exergy-related indicator in performance evaluation of the ORCs. As shown in Equation (1), it is calculated based on the net power output P_{out} and the inlet exergy flow rate of the heat carrier $\dot{B}_{hs1}$. This means that, for a given energy source and environmental conditions, the η_{ex} is only a function of parameters that affect P_{out}. For this reason, the η_{ex} can be effectively applied in optimizing the ORC for maximum power production [9]. The interpretation of the η_{ex} is straightforward and intuitive since it compares the generated output (P_{out}) to the utilized resource ($\dot{B}_{hs1}$). However, in the case of open type energy sources, an essential part of the analysis is to examine and evaluate the utilization degree of an energy source and the η_{ex} does not provide that information.

The remaining exergy-based indicators were applied much less often in the previous studies. Xiao et al. [10] conducted a multi-objective optimization to find the optimal evaporation and condensation temperatures for the ORC utilizing waste flue gas as a heat carrier. The authors applied sustainability index *SI* (Equation (2)) as one of the objective functions to minimize the exergy destruction rate $\delta\dot{B}_{tot}$ and maximize the exergy drop of the heat carrier $\Delta\dot{B}_{hs}$. The latter is equivalent to maximize the potential of the heat source. The study results have shown that *SI* is in conflict with a second criterion which was defined as the total investment cost to net power output. For this reason, *SI* may be used for reducing the ORC exergy destruction, but it is not effective in optimizing the system from the economic perspective. Abam et al. [11] examined different low-temperature ORC configurations and applied waste exergy ratio *WER* (Equation (3)) as one of the indicators to evaluate the sustainable performance of the systems. It is worthwhile to note that *WER* includes both types of exergy waste: exergy destruction $\delta\dot{B}_{tot}$ within the system components (turbine, condenser, pump, vapor generator) and exergy loss $\delta\dot{B}_{loss}$ to the environment. The latter is mainly caused by the high temperature of the heat carrier discharged to the surroundings. This type of exergy waste is expressed as the outlet exergy flow of the heat source $\dot{B}_{hs2}$. It means that by minimizing *WER*, $\dot{B}_{hs2}$ is also minimized leading to maximization of the heat source potential. As noted by Aydin [12], *WER* is a

useful index in improving the sustainable and environmentally friendly work of the energy systems. Furthermore, a physical meaning of *WER* is also easy to understand since it compares the overall exergy waste in the system to the input exergy of the heat source. Environmental effect factor *EEF* (Equation (4)) was considered in the study by Abam et al. [13]. The researchers examined three working fluids (R1234ze, R1234yf, R245fa) and used the *EEF* to assess the sustainability and environmental impact of several ORC architectures. In the same study, the exergetic sustainability index *ESI* (Equation (5)) was applied for the same purpose and the authors found that R245fa provides the most sustainable work. An application of *EEF* and *ESI* was also reported in the article by Midilli and Dincer [14]. The authors used the indicators to examine the recirculating aquaculture system and noted that with an increase of exergy waste ratio *WER* both the exergy efficiency η_{ex} and *ESI* decreased, while the *EEF* increased. Such a relationship is clear since both indices (*EEF* and *ESI*) are defined based on the *WER* and exergy efficiency η_{ex} (see Equations (1)–(5)). Despite the fact that *EEF* and *ESI* can also be applied for enhancing the sustainable operation of the ORC, their formulations are more complex and do not have a straightforward interpretation as the exergy efficiency η_{ex} or waste exergy ratio *WER*.

Certainly, the aforementioned exergy-related indicators, which were investigated by multiple authors, are efficient in maximizing the utilization of the energy source to some extent. However, to the best of the authors knowledge, there is no index, that would combine the simple form of the effectiveness indicator ε and simultaneously, would be based on the exergy balance equation. The role of the latter is particularly important within the context of the utilization of waste energy streams. Therefore, a novel exergy-based indicator is proposed in the current study and the performance analysis of the ORC is conducted in order to compare it with the commonly known ORC parameters and indices. Furthermore, the potential of the proposed index to be a significant performance indicator is revealed, using it as one of the objective functions in multi-objective optimization of the system.

The selected exergy-related indicators are formulated for basic ORC in Equations (1)–(5).

Exergy efficiency

$$\eta_{ex} = \frac{P_{out}}{\dot{B}_{hs1}} \cdot 100\% \tag{1}$$

Sustainibility index

$$SI = \frac{\delta \dot{B}_{tot}}{\Delta \dot{B}_{hs}} \tag{2}$$

Waste exergy ratio

$$WER = \frac{\delta \dot{B}_{tot} + \delta \dot{B}_{loss}}{\dot{B}_{hs1}} \cdot 100\% \tag{3}$$

Environmental effect factor

$$EEF = \frac{WER}{\eta_{ex}} \tag{4}$$

Exergetic sustainiblity index

$$ESI = \frac{1}{EEF} \tag{5}$$

2. System Description

The system examined in the study is modelled as basic subcritical ORC power plant. The turbine, condenser, pump and vapor generator are considered as component parts of the system. The working fluid of the ORC is of an organic origin and it is characterized by lower saturation temperatures (less than 100 °C at suitable pressure levels) than in the classical power plant using water (up to 540 °C). For the studied case, R1234ze is selected as one of the most perspective fluids, which is reflected in the low level of its environmental indicators: *GWP* = 6 and *ODP* = 0 [15]. The low evaporation temperature t_{eva} of the fluid allows for the application of a low-temperature energy source. In this study, geothermal water is used as a heat carrier (Figure 1).

The working fluid of the ORC undergoes the thermodynamic processes in each component of the system. In vapor generator, preheating to saturated liquid state (7–8), evaporation to saturated vapor state (8–9) and superheating (9–1) of the fluid take place. Then, the process of expansion (1–5) in the turbine allows to produce the useful work on the shaft. After cooling (5–5″) and condensing (5″–6) in the condenser, the fluid goes to the pump, in which it is compressed (6–7) from low to high-pressure and the cycle is repeated.

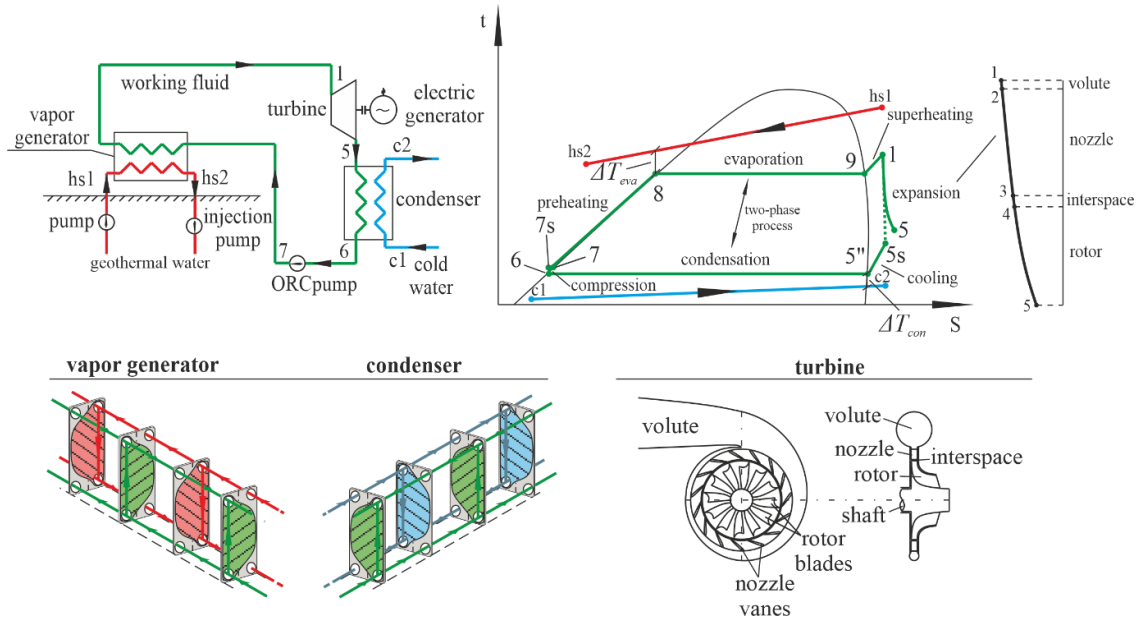

Figure 1. ORC system and modelling assumptions.

The heat exchangers of the ORC, i.e., the vapor generator and condenser, are modelled as plate heat exchangers. The high heat transfer efficiency, compactness and flexibility make them an optimal choice for the considered system. The ORC expansion device is modelled as single-stage radial-inflow turbine (RIT) which proved to work efficiently for small-scale electricity production [16]. The RIT components that are included in the analysis of the study are presented in Figure 1. During the flow through the volute and nozzle, the working fluid is accelerated, and then, flowing through the rotor blades, its kinetic energy is converted into useful work.

The assumed values of the ORC parameters are tabulated in Table 1. The energy source parameters, i.e., the inlet temperature of the hot water t_{hs1} and volume flow rate $\dot{V}_{hs}$, are held constant. The value of the t_{hs1} is typical for low-temperature geothermal energy resources [17]. The temperature difference ΔT_{eva} between the heat carrier and working fluid at the saturated liquid point (point 8 in Figure 1) and the temperature difference ΔT_{con} between the working fluid and cold water at the saturated vapor point (point 5″ in Figure 1) are assumed as in [18]. As suggested in [19], slight superheating degree, expressed as: ΔT_{sup}, is recommended for the ORC. The evaporation t_{eva} and condensation t_{con} temperatures of the working fluid along with the specific speed n_s of the turbine are selected as the decision variables. The latter quantity is defined by the following equation:

$$n_s = \frac{\omega \dot{V}_{05}^{0.50}}{\Delta H_{is}^{0.75}} \tag{6}$$

where ω denotes rotation speed of the rotor [rad s^{-1}], ΔH_{is} refers to the isentropic enthalpy drop of the working fluid [kJ kg^{-1}]. The turbine efficiency η_T is an initial guess, since the exact value is calculated after RIT design which is briefly discussed in Section 4.

Table 1. Parameters and variables of ORC.

Note	Parameter	Unit	Value
constant value	$\dot{V}_{hs}$	[m^3 h^{-1}]	30.0
	t_{hs1}	[°C]	120
	fluid	[-]	R1234ze
	ΔT_{sup}	[K]	5.00
	ΔT_{con}	[K]	5.00
	t_{c1}	[°C]	15.0
	η_P	[-]	0.75
	ΔT_{eva}	[K]	5.00
	T_r	[K]	288.15
decision variables	t_{eva}	[°C]	60.0 ÷ 100
	t_{con}	[°C]	25.0 ÷ 40.0
	n_s	[-]	0.40 ÷ 0.70
initial guess	η_T	[-]	0.75

3. Definition of *XUI*

The exergy balance equation for the analyzed ORC system can be written in the following form:

$$\dot{B}_{hs1} = P_{out} + \delta\dot{B}_{tot} + \dot{B}_{c2} + \dot{B}_{hs2} \tag{7}$$

where $\dot{B}_{hs1}$ and $\dot{B}_{hs2}$ are the exergy flow rates of the heat carrier at the inlet and outlet of the vapor generator, $\dot{B}_{c2}$ is the exergy flow rate of the cold water at the outlet of the condenser, and $\delta\dot{B}_{tot}$ is the total internal exergy destruction rate in the system. The latter is the sum of exergy destruction rates in all considered ORC components. The exergy flow rate of the cold water at the inlet of the condenser $\dot{B}_{c1}$ is equal to zero since at this state the cold water is at the reference conditions. The general equation for the exergy flow rate $\dot{B}$ of the fluid at state x is the following:

$$\dot{B}_x = \dot{m}[h_x - h_r - T_r(s_x - s_r)] \tag{8}$$

where subscript r denotes that the enthalpy h and entropy s are determined at the reference state.

Let's write the Equation (7) in the alternate form:

$$\Delta\dot{B}_{hs} = P_{out} + \delta\dot{B}_{tot} + \dot{B}_{c2} \tag{9}$$

In order to maximize the energy utilization of the heat carrier (geothermal water), the exergy drop $\Delta\dot{B}_{hs}$ should be maximized or, equivalently, the exergy flow rate $\dot{B}_{hs2}$ should be minimized. Theoretically, the maximum allowable exergy potential of the energy source would be utilized if $\dot{B}_{hs2} = 0$, which also means: $\Delta\dot{B}_{hs} = \dot{B}_{hs1}$. The proposed indicator, called exergy utilization index, is defined as follows:

$$XUI = \frac{\Delta\dot{B}_{hs}}{\dot{B}_{hs1}} \cdot 100\% \tag{10}$$

or in the alternate form:

$$XUI = \left(1 - \frac{\dot{B}_{hs2}}{\dot{B}_{hs1}}\right) \cdot 100\% \tag{11}$$

As seen in Equation (10), the *XUI* compares the exergy drop $\Delta\dot{B}_{hs}$ of the heat carrier with the exergy flow rate $\dot{B}_{hs1}$. Based on the definition of *XUI* and aforementioned statements, the following relationships can be written:

$$\Delta\dot{B}_{hs} \to \dot{B}_{hs1} \Longrightarrow XUI \to 100\% \tag{12}$$

$$\Delta\dot{B}_{hs} \to 0 \Longrightarrow XUI \to 0\% \tag{13}$$

The implications given in Equations (12)–(13) reflect the simple structure and straightforward meaning of the proposed indicator. Specifically, the maximization of the energy source utilization expressed in Equation (12) leads to maximization of the *XUI*. For the opposite case, Equation (13), a poor utilization of the energy source corresponds to the value of *XUI* that goes to 0%.

4. Calculation Model

The model of the ORC power plant was developed using MATLAB [20] environment and the original code was written in order to perform the analysis of the exergy utilization index *XUI* and conduct multi-objective optimization by applying the proposed indicator.

4.1. Assumptions

The basic assumption in the modelling of the ORC is to consider each component as the control volume. Then, mass, energy, and exergy balance equations can be applied to determine dependent parameters of the ORC. Furthermore, the following simplifications are introduced in the model:

- the system operates at steady state conditions,
- the changes in the kinetic and potential energy of the fluids are neglected, except for the turbine, in which the kinetic energy of the working fluid is included in the analysis,
- the pressure drops in the connecting pipes and heat exchangers are neglected,
- the heat losses to the environment are ignored,
- the efficiency of the pump η_P is a constant value.

4.2. Algorithm and Research Tools

The algorithm presented in Figure 2 starts from assigning the values to the constant ORC parameters (assumed parameters) and setting the bounds for the decision variables. Then, applying the assumptions described in Section 4.1, basic thermodynamic and heat transfer parameters are calculated (Equations (14)–(16) and (19)). The properties of the fluids (specific enthalpies, specific entropies etc.) are evaluated using the REFPROP database [21]. In the next step, design of the radial-inflow turbine (RIT) is implemented using one-dimensional model [16] which is perceived to be an optimal approach in the preliminary analysis. Moreover, the total-to-static efficiency of the turbine is calculated (Equation (17)) applying the enthalpy loss correlations. The calculation of the selected ORC operating parameters and performance indicators (Equations (23)–(25)) is made in the next step. After that, the multi-objective optimization problem is defined and solved, using non-dominated sorting genetic algorithm-II (NSGA-II) [22], the optimization tool that is embedded in MATLAB. When the optimal solutions are determined, the results are displayed in the form of a Pareto frontier and the calculation procedure is ended.

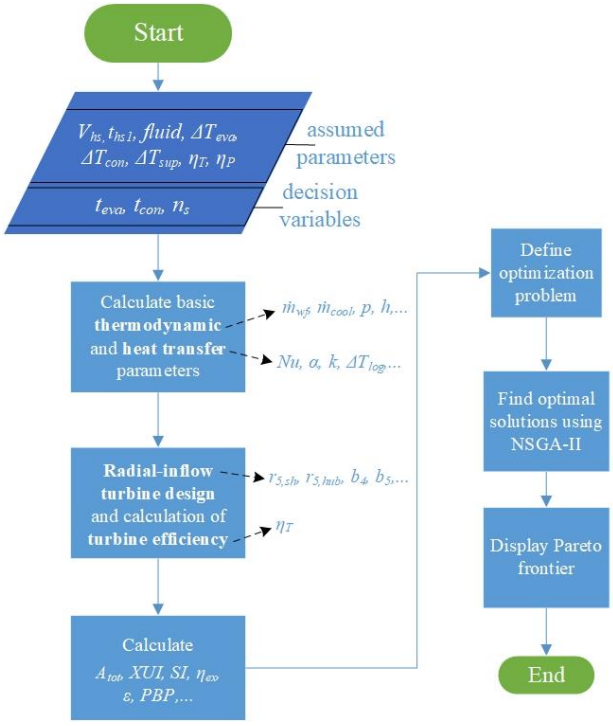

Figure 2. Flowchart of calculation procedure.

4.2.1. Thermodynamic Analysis

Due to the great amount of equations used in the model of the ORC, it was decided to present the relationships only for the selected parameters and performance indicators. The energy balance equations that were used to calculate the mass flow rates of the working fluid $\dot{m}_{wf}$ and cold water $\dot{m}_{cool}$ have the following forms:

$$\rho_{hs}\dot{V}_{hs}c_{hs}[t_{hs1} - (t_{eva} + \Delta T_{eva})] = \dot{m}_{wf}(h_1 - h_8) \tag{14}$$

$$\dot{m}_{wf}(h_{5''} - h_6) = \dot{m}_{cool}c_{cool}[(t_{con} - \Delta T_{con}) - t_{c1}] \tag{15}$$

The temperature of the geothermal water t_{hs2} at the outlet of the vapor generator is calculated using equation:

$$t_{hs2} = t_{hs1} - \frac{\dot{m}_{wf}(h_1 - h_7)}{\rho_{hs}\dot{V}_{hs}c_{hs}} \tag{16}$$

4.2.2. Radial-Inflow Turbine Design

The turbine total-to-static efficiency η_T is calculated iteratively based on the results of the radial-inflow turbine design and enthalpy loss Δh_{loss} correlations. For a detailed description of the procedures similar to the model applied in this study, see [16,23] or some recent papers [24,25]. The general equation used to calculate η_T is the following:

$$\eta_T = 1 - \frac{\sum \Delta h_{loss}}{h_{01} - h_{5s}} \tag{17}$$

The total enthalpy h_{01} at the volute inlet is the enthalpy of the fluid at state 1 (see Figure 1) increased by a kinetic energy at the inlet of the volute:

$$h_{01} = h_1 + \frac{c_1^2}{2} \tag{18}$$

4.2.3. Heat Transfer Analysis

The most significant outcome of the heat transfer analysis is the total heat transfer area A_{tot} which is the sum of the heat transfer areas of the vapor generator and condenser. In general, the logarithmic mean temperature difference ΔT_{log} method was applied in order to calculate the individual heat transfer areas and the following equation was used:

$$A = \frac{\dot{Q}}{k\Delta T_{log}} \tag{19}$$

The above-mentioned method is applied for the individual sections of the heat exchangers. The vapor generator is divided into preheating, evaporating and superheating sections, while in the condenser, the sections of cooling and condensing of the working fluid are distinguished. The heat fluxes $\dot{Q}$ for each section are determined based on the energy balance equations similar to these presented in Equations (14)–(15)).

The formula for determining the overall heat transfer coefficient k is the following:

$$k = \left(\frac{1}{\alpha_{hot}} + \frac{\delta}{\lambda_p} + \frac{1}{\alpha_{cold}}\right)^{-1} \tag{20}$$

The quantities characterizing heat exchanger plates, i.e., their width δ and thermal conductivity λ_p are assumed to be equal to 0.60 mm and 18.0 W m^{-1} K^{-1}. The heat transfer coefficients α are determined for the hot and cold side of a plate. The hot site relates to the fluid which releases heat while the cold site corresponds to the medium which absorbs the energy. The coefficients α are calculated based on the value of Nusselt number Nu and the following equation is applied:

$$\alpha = \frac{Nu\lambda_l}{d_h} \tag{21}$$

The λ_l denotes thermal conductivity of a medium, while d_h is a hydraulic diameter calculated as double distance h_0 between heat exchanger plates. The h_0 is assumed to be equal 1.50 mm. To calculate the Nu, empirical correlations developed for plate heat exchangers and specific processes (condensation, evaporation etc.) are applied and the full list of utilized equations was presented in the previous study [26].

The logarithmic mean temperature difference ΔT_{log} is calculated as:

$$\Delta T_{log} = \frac{T_{hot,in} - T_{cold,out} - \left(T_{hot,out} - T_{cold,in}\right)}{ln\left(\frac{T_{hot,in} - T_{cold,out}}{T_{hot,out} - T_{cold,in}}\right)} \tag{22}$$

The subscripts *hot,in* and *hot,out* indicate that the temperatures are determined for the hot side at the inlet and outlet of a specific heat exchanger section. The same meaning relates to subscripts *cold,in* and *cold,out*.

4.2.4. ORC Performance Indicators

The net power output P_{out} is calculated using the following formula:

$$P_{out} = \dot{m}_{wf}\left[\eta_T(h_{01} - h_{5s}) - \frac{h_{7s} - h_6}{\eta_P}\right] \tag{23}$$

The effectiveness ε indicator is defined as follows:

$$\varepsilon = \frac{t_{hs1} - t_{hs2}}{t_{hs1} - t_r} \cdot 100\% \tag{24}$$

The assumed value of the reference (environmental) temperature is equal to: t_r = 15.0 °C.

The economic aspect is of great importance in the optimization of the ORC systems, since it allows to exclude the operating parameters that would lead to high cost of the installation. In the current study, payback period *PBP* is applied and calculated using the following formula [27]:

$$PBP = \frac{ln\left(\frac{P_{out}C_{el}t_{op} - COM_cC_{tot}}{P_{out}C_{el}t_{op} - COM_cC_{tot} - i_rC_{tot}}\right)}{ln(1+i_r)} \quad (25)$$

The following values of the electricity price, operating time, cost of operation and maintenance coefficient and interest rate are assumed: C_{el} = 0.15 \$ kWh^{-1}, t_{op} = 8000 h, COM_c = 1.50% and i_r = 5.00%. Their values are similar to those adopted in [27].

The capital cost C_{tot} is determined by adding the costs of individual ORC components:

$$C_{tot} = (C_{VG} + C_C + C_T + C_P)\frac{CEPCI_{2018}}{CEPCI_{1996}} \quad (26)$$

The cost of a single component *C* is determined using equation:

$$C = C_{PEC}F_{BM} \quad (27)$$

The purchased equipment cost C_{PEC} is estimated from:

$$logC_{PEC} = K_1 + K_2log(Z) + K_3[log(Z)]^2 \quad (28)$$

Since the purchased equipment costs C_{PEC} for various technical facilities were estimated in 1996, the *CEPCI* (chemical engineering plant cost index) coefficients are adopted in Equation (26) to include an inflation and an increase of material prices. The remaining constant factors which depend on the component type are selected based on recommendations given in [28]. The assumed values of coefficients K_1, K_2, and K_3 are listed in Table 2. The *Z* coefficient is a design parameter for a certain type of component. In the case of a turbine and pump, these are the generated and consumed power, while for the heat exchangers, their heat transfer areas.

Table 2. Coefficients for determining costs of system components.

Component	K_1	K_2	K_3	B_1	B_2	F_m	C_1	C_2	C_3	F_{BM}
Vapor generator and condenser	4.6656	−0.1557	0.1547	0.96	1.21	2.40	0	0	0	-
Turbine	2.6259	1.4398	−0.1776	-	-	-	-	-	-	3.50
Pump	3.3892	0.0536	0.1538	1.89	1.35	1.60	−0.3935	0.3957	-0.00226	-

The bare module coefficient F_{BM} is calculated using equation:

$$F_{BM} = B_1 + B_2F_mF_p \quad (29)$$

For a turbine, the value of F_{BM} is assumed to be equal to 3.5 as suggested by Li et al. [29]. The coefficients B_1 and B_2 depend on the component type, while the F_m is a material factor which takes into account an influence of construction material on the component cost. The assumed values of B_1, B_2 and F_m are tabulated in Table 2. The pressure factor F_p as calculated using the following equation:

$$logF_p = C_1 + C_2log(p) + C_3[log(p)]^2 \quad (30)$$

The coefficients C_1, C_2, and C_3 depend on the component type and their values are listed in Table 2.

4.2.5. Multi-Objective Optimization

The multi-objective optimization problem is defined as follows:

$$minimize: \ f_1(\vec{X}) = -XUI, \quad f_2(\vec{X}) = A_{tot} \tag{31}$$

Subject to :

$$t_{hs2} \geq 60.0^{\circ}\mathrm{C} \tag{32}$$

$$\frac{r_{5,sh}}{r_4} \leq 0.78 \tag{33}$$

$$\frac{r_{5,hub}}{r_{5,sh}} \geq 0.40 \tag{34}$$

$$-40.0^{\circ} \leq inc \leq 0.00^{\circ} \tag{35}$$

$$Ma_4 \leq 1.50 \tag{36}$$

$$Ma_5 \leq 1.00 \tag{37}$$

$$Z_R \geq 1.50 \cdot b_4 \tag{38}$$

$$0.45 \leq R \leq 0.65 \tag{39}$$

The constraint expressed by Equation (32) is imposed in order to avoid silica oversaturation of the geothermal water [30]. The limitations given in Equations (33)–(39) should provide a rational design of the radial-inflow turbine [23]. The $\vec{X}$ represents the vector of decision variables. Their bounds are presented in Table 1.

4.3. Validation of Model

The calculation model has been verified using the results of the study by Da Lio et al. [31]. The outcomes of the basic radial-inflow turbine (RIT) design parameters and turbine efficiency have been compared. The comparative analysis of the findings (Table 3) allows to state that the considered model of the ORC gives reliable results, since the percentage errors are relatively small.

Table 3. Verification of proposed model.

RIT Rotor Geometry	**Fluid: R245fa, $\dot{m}_{wf}$ = 20 kgs^{-1}, t_{eva} = 110 °C, t_{con} = 33 °C, n_s = 0.45**				
	Unit	**Description**	**Present study**	**Da Lio et al. [31]**	**Percentage Error [%]**
r_4	[m]	radius at the rotor inlet	0.195	0.194	0.51
$r_{5,sh}$	[m]	shroud radius at the rotor outlet	0.127	0.133	4.51
$r_{5,hub}$	[m]	hub radius at the rotor outlet	0.058	0.054	7.41
b_4	[m]	blade width at the rotor inlet	0.014	0.015	6.67
b_5	[m]	blade width at the rotor outlet	0.069	0.079	12.7
total-to-static turbine efficiency					
η_T	[%]	turbine efficiency	80.4	86.9	7.48

5. Exergy-Related Indicators

It is worthwhile to share a few insights concerning exergy-related indicators presented in Equations (1)–(5). It should be noted that there are simple relations between the exergy efficiency η_{ex}

and indices given in Equations (3)–(5). Recalling the definition of the η_{ex} (Equation (1)) and exergy balance equation (Equation (7)) for the considered ORC, one can write:

$$\eta_{ex} = \frac{\dot{B}_{hs1} - \delta\dot{B}_{tot} - \dot{B}_{hs2} - \dot{B}_{c2}}{\dot{B}_{hs1}} \tag{40}$$

Let's write the outlet exergy flow rates of the heat source $\dot{B}_{hs2}$ and cold water $\dot{B}_{c2}$ as the exergy loss $\delta\dot{B}_{loss}$ to the environment:

$$\delta\dot{B}_{loss} = \dot{B}_{hs2} + \dot{B}_{c2} \tag{41}$$

After applying Equation (41) in Equation (40) and making simple rearrangements, the exergy efficiency η_{ex} can be written in the following form:

$$\eta_{ex} = 1 - \frac{\delta\dot{B}_{tot} + \delta\dot{B}_{loss}}{\dot{B}_{hs1}} \tag{42}$$

Using the definition of waste exergy ratio *WER* (Equation (3)), it can be identified that:

$$WER = 1 - \eta_{ex} \tag{43}$$

Moreover, since the environmental effect factor *EEF* and exergetic sustainability index *ESI* are both based on the η_{ex} and *WER*, the following relations are derived:

$$EEF = \frac{1 - \eta_{ex}}{\eta_{ex}} \tag{44}$$

$$ESI = \frac{\eta_{ex}}{1 - \eta_{ex}} \tag{45}$$

Based on the equations given above, it can be concluded that the indicators written in Equations (3)–(5) are simple combinations of the exergy efficiency η_{ex}.

6. Results and Analysis

The results of the analysis are presented in Figures 3–11. The graphs in Sections 6.1 and 6.2 are constructed in a similar way, i.e., the *XUI* and selected ORC parameter/indicator are drawn with respect to the evaporation temperature t_{eva} of the working fluid, the parameter that is one of the key variables in performance optimization of the ORC. In Section 6.3, the outcomes of the multi-objective optimization are shown and discussed.

6.1. Relation Between XUI and Selected ORC Parameters

The maximization of the energy utilization in the ORC is inseparably connected with minimizing the outlet temperature t_{hs2} of the heat carrier. Recalling the definition of the *XUI* given in Section 3, the relation between the proposed index and the temperature t_{hs2} should be equivalent. Indeed, the results presented in Figure 3, seem to verify this statement. Specifically, the higher values of the *XUI* correspond to lower outlet temperatures t_{hs2} of the geothermal water. The increase of the t_{hs2} with respect to the t_{eva} can be easily explained using Equation (14) and Equation (16). The increase of the t_{eva} corresponds to decrease of the mass flowrate $\dot{m}_{wf}$ of the working fluid which in turn leads to increase of the t_{hs2}. The fact that *XUI* decreases with an increase of the t_{eva} is mainly due to increase of the t_{hs2}. The higher values of the t_{hs2} correspond to higher specific enthalpies h_{hs2}, which reduces the outlet exergy flow rate $\dot{B}_{hs2}$ of the heat carrier and therefore also the value of *XUI* (Equation (11)). It is worthwhile to mention that, due to the constraint imposed on the t_{hs2} ($t_{hs2} \geq 60°C$), the values of *XUI* higher than ~76% cannot be achieved for the considered case.

The statements given above are verified in Figure 4 which shows that the exergy flow rate $\dot{B}_{hs2}$ increases with an increase of the t_{eva}. Moreover, the opposite relationship between the *XUI* and $\dot{B}_{hs2}$ is confirmed, i.e., the minimization of the latter leads to maximization of the first one.

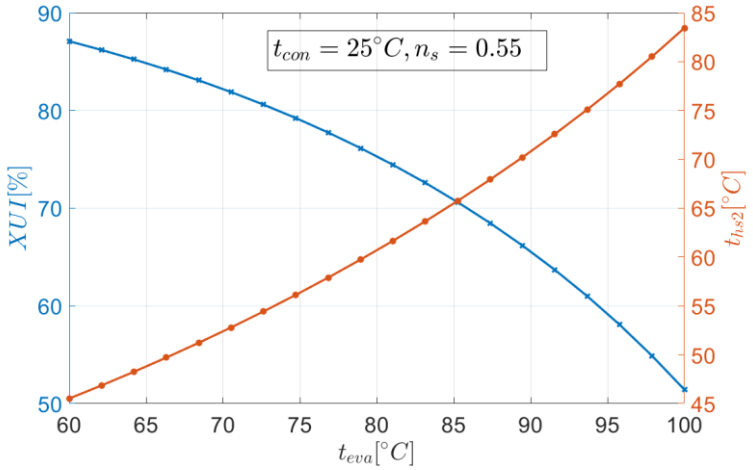

Figure 3. *XUI* and temperature t_{hs2} of the heat carrier at the outlet of vapor generator as functions of evaporation temperature $t_{eva.}$

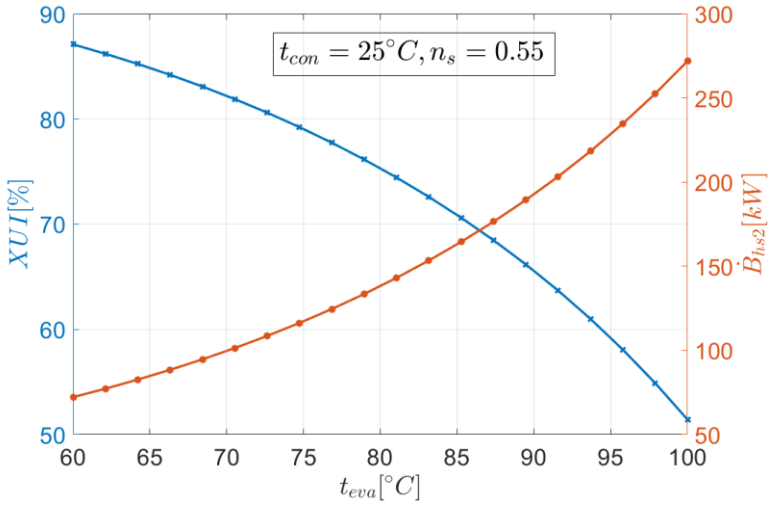

Figure 4. *XUI* and exergy flux $\dot{B}_{hs2}$ of the heat carrier at the outlet of vapor generator as functions of evaporation temperature t_{eva}.

The crucial ORC parameter to be analyzed is the net power output P_{out} and its relationship with the *XUI* is presented in Figure 5. It can be seen that the global maximum of the P_{out} is obtained for the t_{eva} = ~75 °C. The point of the maximum P_{out} corresponds to the high value of the *XUI* which reaches nearly 80%. The higher values of the t_{eva} lead to a decrease of both *XUI* and P_{out}. Considering the fact that values of *XUI* exceeding 80% cannot be obtained for the reasons mentioned above, the maximization of the *XUI* shall ensure the maximization of the P_{out}. The existence of the extremum of the P_{out} is due to the conflicting influence of the t_{eva} on the mass flow rate $\dot{m}_{wf}$ and thermal efficiency η_{ORC} of the ORC.

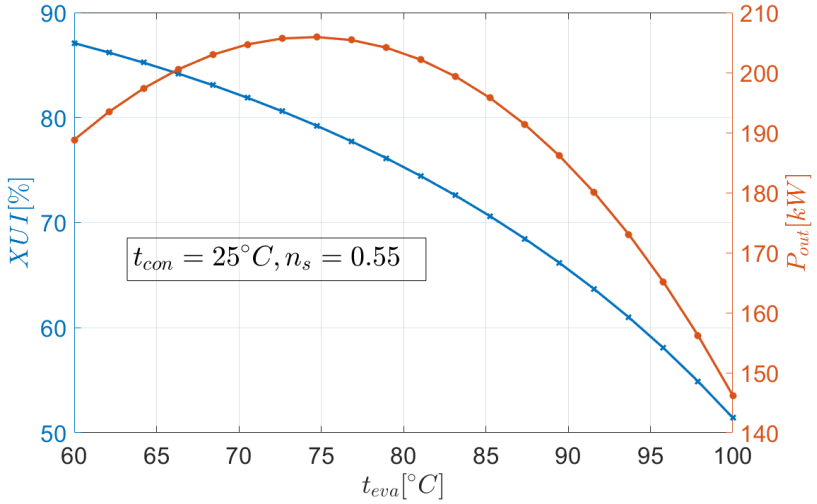

Figure 5. *XUI* and net power output P_{out} as functions of evaporation temperature t_{eva}.

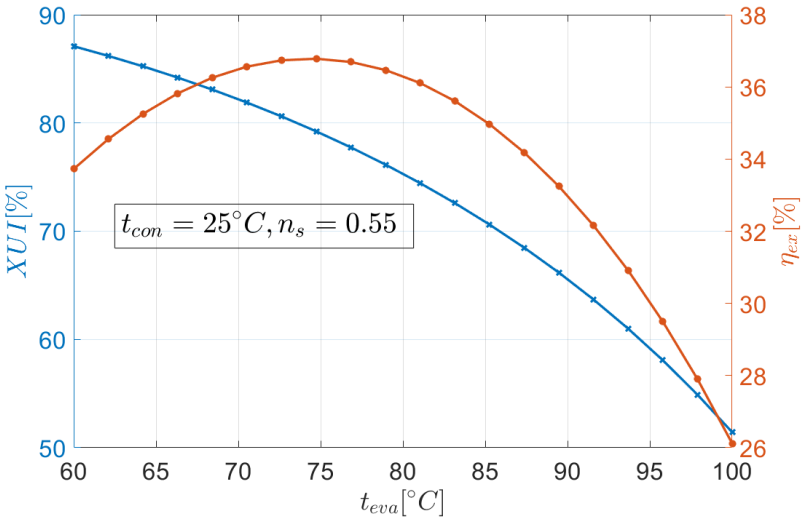

Figure 6. *XUI* and exergy efficiency η_{ex} as functions of evaporation temperature t_{eva}.

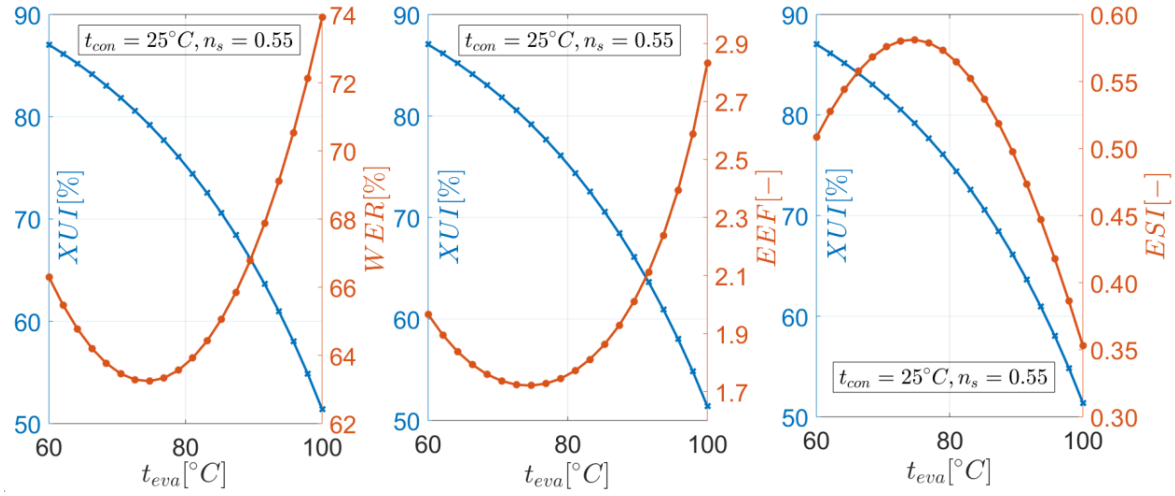

Figure 7. *XUI* and exergy-related indicators as functions of evaporation temperature t_{eva}.

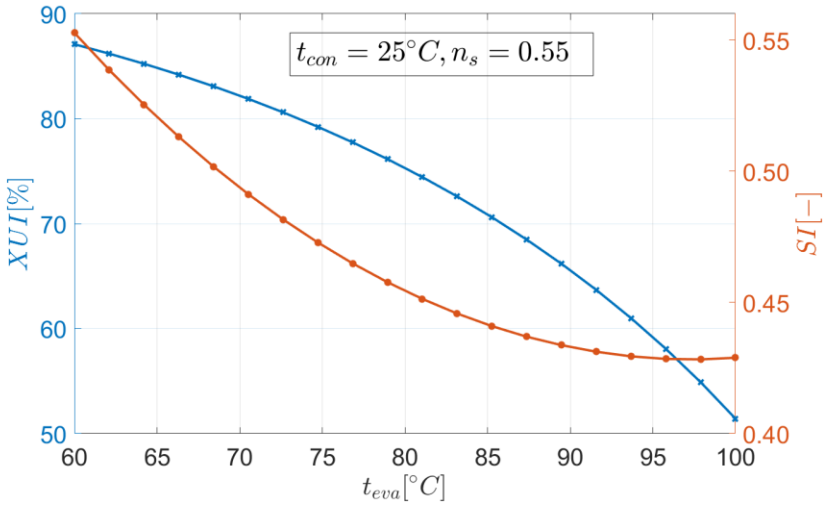

Figure 8. *XUI* and *SI* index as functions of evaporation temperature t_{eva}.

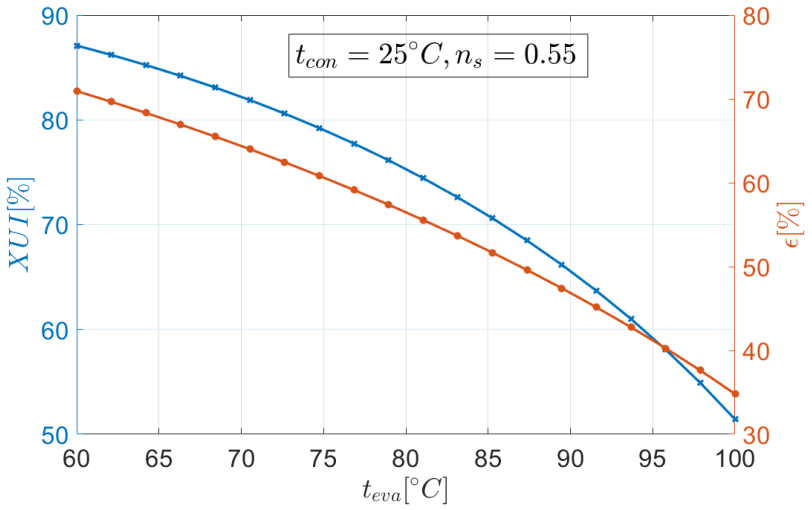

Figure 9. *XUI* and effectiveness index ε as functions of evaporation temperature t_{eva}.

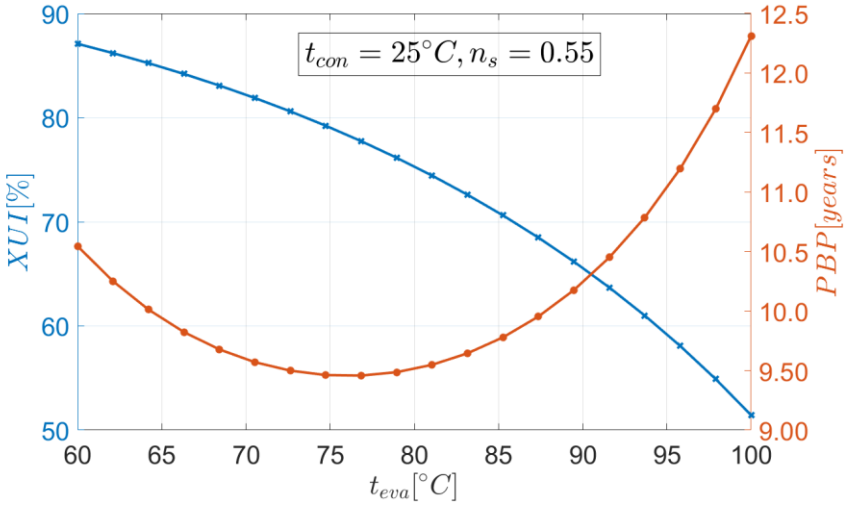

Figure 10. *XUI* and payback period *PBP* as functions of evaporation temperature t_{eva}.

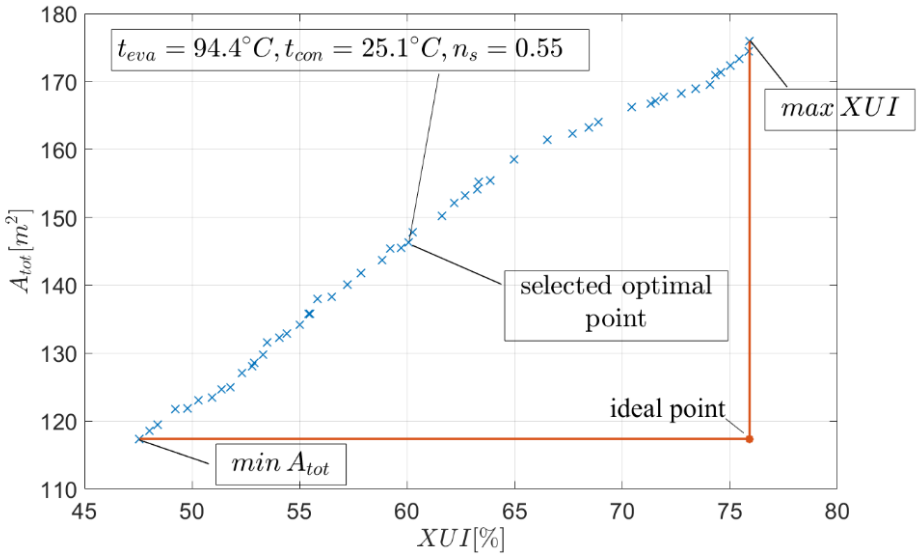

Figure 11. Pareto frontier.

6.2. Comparative Analysis of XUI and Selected ORC Serformance Indicators

In order to reveal the similarities and differences between the *XUI* and common ORC performance indicators, the results for the proposed index are compared with the outcomes obtained for: five exergy-related, one energy-based and one economic indicator. The exergy efficiency η_{ex} is mostly affected by the net power output P_{out} (see Equation (1)). Therefore, the relationship with respect to the evaporation temperature t_{eva} is the same (see Figure 6) as for the P_{out} (see Figure 5). Moreover, the maximization of the *XUI* leads to the higher values of the η_{ex} for the studied case.

In the previous sections, it was discussed that the exergy-related indicators, such as waste exergy ratio *WER*, environmental effect factor *EEF* and exergetic sustainability index *ESI*, are basic combinations of the exergy efficiency η_{ex}. This observation is reflected in the results presented in Figure 7. By comparing the outcomes for the exergy efficiency η_{ex} (Figure 6) with the results obtained for the *WER*, it is clear that they are consistent with respect to relation given in Equation (43). The global minimum of *WER* is obtained for the same evaporation temperature (t_{eva} = ~75 °C) as in case of the global maximum of the η_{ex}. As expected, almost the same trend as in case of *WER* is observed for the *EEF*. For both indicators *WER* and *EEF*, minimum values are desirable. Following the results obtained for the exergetic sustainable index *ESI*, it is apparent that the shape of the curve is very similar to the η_{ex} and the global optimum point is the same. When it comes to compare the results with respect to the exergy utilization index *XUI*, the observations are similar as for the net power output P_{out} and exergy efficiency η_{ex}. The high values of the proposed indicator (*XUI* = ~80%) correspond to global optima of all three exergy-based indices. This means that for the high utilization degree of the heat source, more sustainable work of the system can be provided.

The sustainability index *SI* defined by Equation (2) compares the total exergy destruction rate $\delta\dot{B}_{tot}$ with the exergy drop of the heat carrier $\Delta\dot{B}_{hs}$. Thus, *SI* should be minimized, reducing $\delta\dot{B}_{tot}$ and maximizing $\Delta\dot{B}_{hs}$. The increase of the latter is equivalent to minimize $\dot{B}_{hs2}$, making it similar to the *XUI*. Even though both objectives favor the minimization of the $\dot{B}_{hs2}$, the results presented in Figure 8 show that the *XUI* and *SI* are in conflict. The reason for that is the fact that the greater values of the t_{eva} correspond to lower exergy destruction rate $\delta\dot{B}_{tot}$. The $\delta\dot{B}_{tot}$ seems to be a dominant factor in case of *SI*. In general, the results show that *SI* is an effective indicator for minimizing internal exergy destructions in the ORC system. However, the minimization of that index simultaneously leads to lower utilization degree of the energy source which is reflected in lower values of the *XUI*. It is worth reminding that the exergy flow rate $\dot{B}_{hs2}$ is also regarded as the component of external exergy loss in the ORC [1]. Therefore, *XUI* can be effectively applied for minimizing this type of exergy losses and it seems to

be a better choice than *SI* in that aspect. Furthermore, for cases in which the heat carrier leaving the vapor generator is directed to the environment, the minimization of the $\dot{B}_{hs2}$ is very beneficial from an ecological perspective, since the negative impact of the medium is reduced. This makes *XUI* a promising indicator in terms of the environmental aspect as well.

The effectiveness ε of the heat carrier (Equation (24)) is defined in a way which should maximize the utilization of the energy source in the system. For this reason, the relationships for both *XUI* and ε with respect to the t_{eva} are very similar (Figure 9). The fact that *XUI* includes the entropy generation rate (see Equation (8)) of the heat carrier makes it more comprehensive than ε which is based solely on the energy balance equation.

The economic aspect of the ORC may be examined using different indicators which directly or indirectly evaluate the cost of the installation. In the current study, the payback period *PBP* of the installation is used and results of the calculations are presented in Figure 10. The global minimum of *PBP* is achieved for the evaporation temperature t_{eva} = ~76 °C and the payback period is equal to: *PBP* = ~9.5 years. The location of the extremum is very close to that obtained for the P_{out} which was shown in Figure 5. It suggests that the *PBP* is strongly affected by the net power output P_{out}. The minimum value of the payback period *PBP* corresponds to the high value of the exergy utilization index, i.e.,: *XUI* = ~80%. The significant lower values of the *XUI* (~50%) lead to the noticeable increase of the *PBP* (~12.5 years). The *XUI* values that substantially exceed 80% lead to slight increase in *PBP* (~10.5 years). However, as described in Section 6.1, values of *XUI* greater than 80% cannot be achieved due to the constraint imposed on the outlet temperature t_{hs2} of the heat carrier. Therefore, it can be concluded that maximization of the *XUI* is beneficial with respect to the economic criterion.

6.3. Pareto frontier

The results of the multi-objective optimization using NSGA-II are displayed in the form of a Pareto frontier graph. The Pareto frontier consists of the so-called optimal non-dominated solutions, which means that the improvement of one objective function cannot be made without sacrificing the other one. In order to choose the final optimal solution, a decision-making method should be selected and applied. For the studied case, the ideal point method [32] was used and the result of the decision-making process is presented in Figure 11. The values of the exergy utilization index and total heat transfer area that correspond to the selected optimal point are the following: *XUI* = 60.1% and A_{tot} = 146 m^2.

Recalling the outcomes presented in the previous subsections, the selected optimal value of the *XUI* shall ensure favorable values of the economic (payback period *PBP*) and environmental ($\dot{B}_{hs2}$) indices, exergy efficiency η_{ex} or net power output P_{out}. Simultaneously, the choice of the total heat transfer area A_{tot} as the second objective function allows for maintaining the compactness of the system. The fact that *XUI* is in conflict with the A_{tot} allows to conclude that the proposed indicator is not effective in minimizing the size of the system. This is mainly because the *XUI* is strongly affected by the mass flow rate of working fluid $\dot{m}_{wf}$ and the increase of the latter leads to the continuous increase of the first one. That is also the main reason for the greater internal exergy destruction rate $\delta\dot{B}_{tot}$ associated with a larger value of the *XUI* which was shown using *SI* parameter (see Figure 8). Therefore, the *XUI* can be regarded as the criterion which maximization may lead to the beneficial economic and environmental characteristics. However, the simultaneous significant increase of the system dimensions should be balanced using objective functions, such as: A_{tot}, $\delta\dot{B}_{tot}$, or *SI*. In Table 4, the detailed results of the multi-objective optimization are presented. They include the points marked in Figure 11 which correspond to: minimum total heat transfer area (min A_{tot}), selected optimal point, and maximum exergy utilization index (max *XUI*).

Table 4. Results of the multi-objective optimization.

Type of Quantity	Symbol	Unit	Min A_{tot}	Selected Optimal Point	Max *XUI*
decision variables	t_{eva}	[°C]	100	94.4	76.2
	t_{con}	[°C]	37.7	25.1	31.1
	n_s	[-]	0.53	0.55	0.55
objective functions	*XUI*	[%]	47.6	60.1	75.9
	A_{tot}	[m^2]	117	146	176
ORC parameters	$\dot{m}_{wf}$	[kg s^{-1}]	6.05	7.29	10.6
	η_T	[-]	0.83	0.82	0.83
	t_{hs2}	[°C]	86.6	76.0	60.0
	$\dot{B}_{hs2}$	[kW]	294	224	135
	P_{out}	[kW]	113	170	177
exergy-based indicators	η_{ex}	[%]	20.2	30.4	31.6
	WER	[%]	79.8	69.6	68.4
	EEF	[-]	3.94	2.28	2.17
	ESI	[-]	0.25	0.44	0.46
	$\delta\dot{B}_{tot}$	[kW]	116	144	203
	SI	[-]	0.44	0.43	0.48
energy-based indicator	ε	[%]	31.8	41.9	57.1
economic indicator	*PBP*	[years]	17.0	10.9	11.2

7. Conclusions

The aim of the study was to introduce a novel exergy indicator for maximizing energy utilization in ORC power plant. The exergy utilization index *XUI* was analysed by comparing its relationships with selected ORC parameters and performance indicators. Moreover, an illustrative multi-objective optimization using NSGA-II tool was performed in order to reveal the potential for applying *XUI* as objective function in the performance optimization of ORC power plants. The analysis of the results allowed to draw the following conclusions:

- by maximizing *XUI* to the value of 75.9%, the outlet temperature of a geothermal water t_{hs2} is reduced to the environmental temperature (t_r = 15.0 °C) as close as possible, i.e., to the lowest value (t_{hs2} = 60.0 °C) of the constraint imposed on the t_{hs2}. In other words, the potential of the heat source is maximized by maximizing *XUI*,
- the value of *XUI* = ~80% corresponds to the global optima of exergy-based indices which means that high values of *XUI* may be associated with more sustainable work of the ORC,
- the values of the *XUI* = ~60%–80% lead to good economic characteristics reflected in low values of the payback period *PBP* (<11.3 years),
- the maximization of the *XUI* is beneficial from ecological perspective, since it minimizes the negative impact of the heat carrier on the environment, by reducing the value of outlet exergy flow rate $\dot{B}_{hs2}$,
- the proposed indicator is not effective in minimizing the size of the system and its maximization leads to the total heat transfer area A_{tot} which is 50.4% greater than the value obtained while minimizing A_{tot}.

In general, the *XUI* seems to be a promising indicator in the optimization of the ORC power plant, particularly in multi-objective analysis, in which its drawbacks can be balanced using the opposite criterion.

Author Contributions: Conceptualization, M.J. and A.B.; Data curation, M.J. and A.B.; Methodology, M.J.; Software, M.J.; Validation, M.J.; Writing—original draft preparation, M.J.; Writing—review and editing, M.J. and A.B.; Visualization, M.J.; Supervision, A.B. All authors have read and agreed to the published version of the manuscript.

Funding: The work has been partially financed by Polish National Agency for Academic Exchange for implementation the project entitled "R&D in the field of increasing the efficiency of low temperature geothermal power plants" under the agreement PPN/BEK/2018/1/00408/DEC/1.

Acknowledgments: The authors are pleased to acknowledge the West Pomeranian University of Technology in Szczecin for the support.

Conflicts of Interest: The authors declare no conflict of interest.

Nomenclature

A	heat transfer area, m^2
$\dot{B}$	exergy flow rate, kW
b	blade width, m
C_{el}	electricity price, \$ kWh^{-1}
C_{tot}	capital cost, \$
COM_c	cost of operation and maintenance coefficient, %
c	specific heat capacity, kJ kg^{-1} K^{-1}
d_h	hydraulic diameter, mm
EEF	environmental effect factor, -
ESI	exergetic sustainability index, -
h	specific enthalpy, kJ kg^{-1}
inc	incidence angle, °
i_r	interest rate, %
k	overall heat transfer coefficient, W m^{-2} K^{-1}
Ma	Mach number, -
$\dot{m}$	mass flow rate, kg s^{-1}
Nu	Nusselt number, -
n_s	specific speed, -
P_{out}	net power output, kW
PBP	payback period, years
p	pressure, kPa
q	pitch, m
R	reaction degree, -
r	radius, m
SI	sustainability index, -
s	specific entropy, kJ kg^{-1} K^{-1}
T	temperature, K
t	temperature, °C
t_{op}	operating time, h
$\dot{V}$	volume flow rate, m^3 h^{-1}
WER	waste exergy ratio, %
XUI	exergy utilization index, %
Z_R	axial length of rotor, m

Greek Letters

α	heat transfer coefficient, W m^{-2} K^{-1}
$\Delta\dot{B}$	exergy difference, kW
ΔH_{is}	isentropic enthalpy drop, kJ kg^{-1}
Δh_{loss}	enthalpy loss, kJ kg^{-1}
ΔT	temperature difference, K
δ	width of plate, mm
$\delta\dot{B}$	exergy destruction rate, kW
η	efficiency, %
λ	thermal conductivity W m^{-1} K^{-1}
ρ	density, kg m^{-3}
ε	effectiveness, %
ω	angular velocity, rad s^{-1}

Subscript

BM	bare module
C	condenser
con	condensation
cool	cold water
eva	evaporation
ex	exergy
hs	heat source
hub	hub
l	liquid
log	logarithmic
m	material
P	pump
PEC	purchased equipment cost
p	plate or pressure
r	reference state
sh	shroud
sup	superheating
T	turbine
tot	total
VG	vapor generator
wf	working fluid

Abbreviations

CEPCI	chemical engineering plant cost index
GWP	global warming potential
ODP	ozone depletion potential
ORC	organic Rankine cycle

References

1. Borsukiewicz-Gozdur, A. Exergy analysis for maximizing power of organic Rankine cycle power plant driven by open type energy source. *Energy* **2013**, *62*, 73–81. [CrossRef]
2. Li, J.; Ge, Z.; Duan, Y.; Yang, Z. Design and performance analyses for a novel organic Rankine cycle with supercritical-subcritical heat absorption process coupling. *Appl. Energy* **2019**, *235*, 1400–1414. [CrossRef]
3. Gong, M.; Wall, G. On exergy and sustainable development–Part 2: Indicators and methods. *Exergy Int. J.* **2001**, *1*, 217–233. [CrossRef]
4. Garg, P.; Orosz, M.S. Economic optimization of Organic Rankine cycle with pure fluids and mixtures for waste heat and solar applications using particle swarm optimization method. *Energy Convers. Manag.* **2018**, *165*, 649–668. [CrossRef]
5. Li, J.; Ge, Z.; Duan, Y.; Yang, Z.; Liu, Q. Parametric optimization and thermodynamic performance comparison of single-pressure and dual-pressure evaporation organic Rankine cycles. *Appl. Energy* **2018**, *217*, 409–421. [CrossRef]
6. Romero, J.C.; Linares, P. Exergy as a global energy sustainability indicator. A revew of the state of the art. *Renew. Sustain. Energy Rev.* **2014**, *33*, 427–442. [CrossRef]
7. Lecompte, S.; Huisseune, H.; van den Broek, M.; Vanslambrouck, B.; De Paepe, M. Review of organic Rankine cycle (ORC) architectures for waste heat recovery. *Renew. Sustain. Energy Rev.* **2015**, *47*, 448–461. [CrossRef]
8. Sun, W.; Yue, X.; Wang, Y. Exergy efficiency analysis of ORC (Organic Rankine Cycle) and ORC-based combined cycles driven by low-temperature waste heat. *Energy Convers. Manag.* **2017**, *135*, 63–73. [CrossRef]
9. Lecompte, S.; Ameel, B.; Ziviani, D.; van den Broek, M.; De Paepe, M. Exergy analysis of zeotropic mixtures as working fluids in Organic Rankine Cycles. *Energy Convers. Manag.* **2014**, *85*, 727–739. [CrossRef]
10. Xiao, L.; Wu, S.Y.; Yi, T.T.; Liu, C.; Li, Y.R. Multi-objective optimization of evaporation and condensation temperatures for subcritical organic Rankine cycle. *Energy* **2015**, *83*, 723–733. [CrossRef]

11. Abam, F.I.; Ekwe, E.B.; Effiom, S.O.; Ndukwu, M.C.; Briggs, T.A.; Kadurumba, C.H. Optimum exergetic performance parameters and thermo-sustainability indicators of low-temperature modified organic Rankine cycles (ORCs). *Sustain. Energy Technol.* **2018**, *30*, 91–104. [CrossRef]
12. Aydin, H. Exergetic sustainability analysis of LM6000 gas turbine power plant with steam cycle. *Energy* **2013**, *57*, 766–774. [CrossRef]
13. Abam, F.I.; Ekwe, E.B.; Effiom, S.O.; Ndukwu, M.C. A comparative performance analysis and thermo-economic sustainability indicators of modified low-heat organic Rankine cycles (ORCs): An exergy-based procedure. *Energy Rep.* **2018**, *4*, 110–118. [CrossRef]
14. Midilli, A.; Kucuk, H.; Dincer, I. Environmental and sustainability aspects of a recirculating aquaculture system. *Environ. Prog. Sustain.* **2011**, *31*. [CrossRef]
15. Vivian, J.; Manete, G.; Lazzaretto, A. A general framework to select working fluid and configuration of ORCs for low-to-medium temperature heat sources. *Appl. Energy* **2015**, *156*, 727–746. [CrossRef]
16. Aungier, R.H. *Turbine Aerodynamics*; ASME Press: New York, NY, USA, 2006.
17. World Energy Council. *World Energy Resources*; World Energy Council: London, UK, 2013; Available online: https://www.worldenergy.org/assets/images/imported/2013/09/Complete_WER_2013_Survey.pdf (accessed on 1 March 2020).
18. Shengjun, Z.; Huaixin, W.; Tao, G. Performance comparison and parametric optimization of subcritical Organic Rankine Cycle (ORC) and transcritical power cycle system for low-temperature geothermal power generation. *Appl. Energy* **2011**, *88*, 2740–2754. [CrossRef]
19. Quoilin, S.; Declaye, S.; Tchanche, B.F.; Lemort, V. Thermo-economic optimization of waste heat recovery Organic Rankine Cycles. *Appl. Therm. Eng.* **2011**, *31*, 2885–2893. [CrossRef]
20. The MathWorks Inc. *MATLAB version R2019a*; The MathWorks Inc.: Natick, MA, USA, 2019.
21. Lemmon, E.W.; Huber, M.L.; McLinden, M.O. *NIST Standard Reference Database 23: Reference Fluid Thermodynamic and Transport Properties-REFPROP, Version 9.1*; National Institute of Standards and Technology: Gaithersburg, MD, USA, 2013.
22. Deb, K.; Pratap, A.; Agarwal, S.; Meyarivan, T. A Fast and Elitist Multiobjective Genetic Algorithm: NSGA-II. *IEEE Trans. Evol. Comput.* **2002**, *6*, 182–197. [CrossRef]
23. Whitfield, A.; Baines, N.C. *Design of Radial Turbomachines*; Longman Scientific & Technical: New York, NY, USA, 1990.
24. Bekiloğlu, H.E.; Bedir, H.; Anlaş, G. Multi-objective optimization of ORC parameters and selection of working fluid using preliminary radial inflow turbine design. *Energy Convers. Manag.* **2019**, *183*, 833–847. [CrossRef]
25. Bahadormanesh, N.; Rahat, S.; Yarali, M. Constrained multi-objective optimization of radial expanders in organic Rankine cycles by firefly algorithm. *Energy Convers. Manag.* **2017**, *148*, 1179–1193. [CrossRef]
26. Jankowski, M.; Borsukiewicz, A. Multi-objective approach for determination of optimal operating parameters in low-temperature ORC power plant. *Energy Convers. Manag.* **2019**, *200*, 112075. [CrossRef]
27. Zhang, C.; Liu, C.; Wang, S.; Xu, X.; Li, Q. Thermo-economic comparison of subcritical organic Rankine cycle based on different heat exchanger configurations. *Energy* **2017**, *123*, 728–741. [CrossRef]
28. Turton, R.; Bailie, R.C.; Whiting, W.B.; Shaeiwitz, J.A. *Analysis, Synthesis and Design of Chemical Processes*; Pearson Education: London, UK, 2009; ISBN 0–13-512966-4.
29. Li, T.; Meng, N.; Liu, J.; Zhu, J.; Kong, X. Thermodynamic and economic evaluation of the organic Rankine cycle (ORC) and two-stage series organic Rankine cycle (TSORC) for flue gas heat recovery. *Energy Convers. Manag.* **2019**, *183*, 816–829. [CrossRef]
30. Liu, C.; Gao, T. Off-design performance analysis of basic ORC, ORC using zeotropic mixtures and composition-adjustable ORC under optimal control strategy. *Energy* **2019**, *171*, 96–108. [CrossRef]
31. Da Lio, L.; Manete, G.; Lazzaretto, A. A Mean-line model to predict the design efficiency of radial inflow turbines in organic Rankine cycle (ORC) systems. *Appl. Energy* **2017**, *205*, 187–209. [CrossRef]
32. Cui, Y.; Geng, Z.; Zhu, Q.; Han, Y. Review: Multi-objective optimization methods and application in energy saving. *Energy* **2017**, *125*, 681–704. [CrossRef]